Influence of the protein and DFT method on the broken-symmetry and spin states in nitroge

Cao, Lili; Ryde, Ulf

Published in:
International Journal of Quantum Chemistry

DOI:
10.1002/qua.25627

2018

Document Version:
Peer reviewed version (aka post-print)

Influence of the protein and DFT method on the broken-symmetry and spin states in nitrogenase

Lili Cao & Ulf Ryde *

Department of Theoretical Chemistry, Lund University, Chemical Centre, P. O. Box 124, SE-221 00 Lund, Sweden

Correspondence to Ulf Ryde, E-mail: Ulf.Ryde@teokem.lu.se, Tel: +46 – 46 2224502, Fax: +46 – 46 2228648

2018-02-19

Abstract

The enzyme nitrogenase contains a complicated $MoFe_7CS_9$ cofactor with 35 possible broken-symmetry (BS) states. We have studied how the energies of these states depend on the geometry, the surrounding protein, the DFT functional and the basis set, studying the resting state, a one-electron reduced state and a protonated state. We find that the effect of the basis set is small, up to 11 kJ/mol. Likewise, the effect of the surrounding protein is restricted, up to 10 and 7 kJ/mol for the electrostatic and van der Waals energy terms. Single-point energies calculated on a single geometry give a good correlation (R^2 = 0.92–0.98) to energies calculated after geometry optimisation, but some BS states may be disfavoured by up to 37 kJ/mol. A change from the pure TPSS functional to the hybrid B3LYP functional may change the relative energies by up to 58 kJ/mol and the correlation between the two results is only 0.57–0.72. Both functionals agree that BS7 is the most stable BS state and that the ground spin state is the quartet for the resting state and the quintet for the reduced state. With the TPSS functional, the BS6 state is the second most stable state, always at least 21 kJ/mol less stable than the BS7 state. However, with the B3LYP functional, BS10 is the second most stable state and for the protonated state it comes close in energy. Based on these results, we suggest a procedure how to consider the 35 BS states in future investigations of the nitrogenase reaction mechanism.

Key Words: nitrogenase; broken-symmetry density functional theory; QM/MM; basis set; functional

Introduction

Nitrogenase (EC 1.18/19.6.1) is one of the most important proteins in nature, being the only enzyme that can cleave the strong triple bond in N_2, reducing it to two molecules of ammonia.[1–3] This is a very demanding reaction, consuming 16 molecules of ATP. Functional nitrogenase is a large complex of two proteins, the Fe protein that provides electrons and the MoFe protein that performs the reduction of N_2. The latter contains two unique cofactors.[4–8] The P cluster is a $Fe_8S_7Cys_6$ assembly, consisting essentially of two merged 4Fe–4S clusters. It is involved in the transport of electrons. The active site consists of the FeMo cluster, a unique $MoFe_7S_9C$ complex, shown in Figure 1. It is connected to the protein by a Cys ligand to one of the Fe ions and a His ligand to the Mo ion. In addition, the Mo ion coordinates bidentately to a homocitrate molecule. In some enzymes, the Mo ion is replaced by a Fe or V ion.[9]

Nitrogenases have been extensively studied by experimental methods.[1–3,10,11] Crystallographic studies have revealed the general structure of the protein and the two clusters,[4] but the central ion of the FeMo cluster was not detected in the early structures and only recently a combination of crystallographic, spectroscopic and computational studies could settle that it is a carbide ion.[5–8,10] Freeze-clamp kinetic experiments have isolated several intermediates in the reaction mechanism[3] and it is normally described as nine states obtained by the consecutive addition of eight electrons and protons to the active site.[12]

Quantum-mechanical (QM) calculations have also been much employed in the study of nitrogenase.[13] Unfortunately, there is no consensus in the detailed mechanism of the enzyme. For example, during 2015 and 2016 one group has suggested that N_2 binds side-on to one Fe ion and is then protonated alternatively on the two N atoms,[14] another that N_2 binds after the dissociation of one of the sulfide ions with one N atom bridging two Fe ions, and the non-coordinating N atom is fully protonated and dissociates before the other N atom is protonated,[15] whereas three groups have suggested that the central carbide ion is involved in the mechanism, either by receiving the incoming protons,[16] or by covalently binding the N_2 substrate in various ways.[17,18] A recent study addressed the role of His-195 in the reaction mechanism.[19]

The QM studies of nitrogenase are obstructed by the complicated nature of the FeMo cluster. Experimentally, it is known to be a spin quartet in the resting state.[3] However, the individual Fe ions are in the high-spin Fe(II) or Fe(III) states, each with four or five unpaired electrons, respectively,[20] and the Mo ion is in the intermediate-spin Mo(III) state.[11] In QM calculations with density-functional theory (DFT), this is normally treated with the broken-symmetry (BS) approach, with separate wavefunctions for electrons of α and β spin. In 2001, Noodleman and coworkers presented a detailed DFT study of the spin states of the FeMo cluster.[20] They, showed that there are 10 BS states for the cluster if it is considered to have C_3 symmetry (35 states without symmetry). These states are schematically depicted in Figure 2. The calculations indicated that one of these states, BS6, gave geometries and calculated spectroscopic parameters closest to experiments. However, these calculations were performed on a FeMo cluster without any central atom. In 2007, calculations were performed with a central atom (N, C or O) and they then found that the BS7 state was lower in energy.[21] BS7 was also found to be the ground state in calculations of an appreciably larger (225-atom) QM-cluster model[11] and it has been used in many recent QM studies of nitrogenase,[10,22–24] although some studies instead used the BS6[14,25] or BS2 states.[16] In calculations that automatically find the lowest BS state, either BS6 or BS7 was found to be the ground state, depending on the oxidation state of the cluster and the bound ligands (substrate and protons) during the reaction mechanism.[26]

Unfortunately, the relative energies of the various spin states depend on the details of the QM calculations. For example, Noodleman showed that the interaction energy with the

surrounding protein and water affects the various BS states differently (by up to 35 kJ/mol); in fact, it changed the predicted ground state from BS2 to BS6.[27] The interaction energy of the three possible BS6 states in the asymmetric protein differed by 8 kJ/mol and a slightly smaller difference (5 kJ/mol) was found for the three BS7 states in a recent QM/MM study.[24] Moreover, different DFT functionals gave spin densities on the Fe ions that differed by over 0.6.[11] Using the B3LYP* functional, Siegbahn reported that the doublet is 17 kJ/mol lower in energy than the quartet for the resting state, modelled by the BS2 state (contrary to the experimental finding of the quartet state).[16] He used the singlet and doublet states for all other intermediates in the reaction mechanism (for which experimental information often is not available), whereas Kästner and Blöchl reported higher spin states (triplets–sextets) for all their intermediates.[26]

Clearly it is computationally too demanding to study all 35 BS states for every putative intermediate in the reaction mechanism in nitrogenase (for example, there are more than 40 possible protonation sites on the FeMo cluster for each oxidation level). On the other hand, the assumption that a certain spin and BS state is most stable for all intermediates is risky and not supported by available results.[26] Therefore, a practical procedure to deal with the BS-states in QM calculations of nitrogenase is needed. With this aim, we in this paper study systematically all 35 possible BS states of the FeMo cluster in nitrogenase with QM/MM methods for the resting state, as well as a one-electron reduced state and a singly protonated state. For each state, we consider two or three spin states (doublet and quartet for the resting and protonated states and the singlet, triplet and quintet states for the reduced cluster). We examine how the relative energies of BS states are affected by the surrounding protein and solvent, the DFT functional, the basis set and the geometry. Thereby, we obtain information about possible variations of the calculated BS energies for various intermediates in the nitrogenase mechanism, and this allows us to propose how to deal with the BS and spin states in future QM investigations.

Methods

The protein

All calculations were based on the 1.0-Å crystal structure of nitrogenase from *Azotobacter vinelandii* (PDB code 3U7Q).[6] The setup of the protein is identical to that of our previous study of the protein.[28] The entire heterotetramer was included in the calculations, because the various subunits are entangled without any natural way to separate them. No attempt was made to model the missing starting and ending residues of the subunits A and C, whereas subunits B and D are complete and were modelled with charged amino and carboxy terminals. Eight imidazole molecules from the buffer were deleted, as well as two Mg^{2+} on the surface of the protein. On the other hand, the two Ca^{2+} ions were kept, because they are deeply buried in the protein and stabilising the interface between the subunits. All crystal-water molecules were kept in the calculations, except 26 that overlapped with each other or with protein atoms.[28]

The QM calculations were concentrated on the FeMo clusters in the C subunit, because there is a buried imidazole molecule from the solvent rather close to the active site (~11 Å) in the A subunit. The P cluster and the FeMo cluster in subunit A were modelled by MM in the fully reduced and resting states, respectively.[28]

The protonation states of all residues were determined from a detailed study of the hydrogen-bond pattern and the solvent accessibility.[28] It was checked by the PROPKA[29] and Maestro[30] software. All Arg, Lys, Asp, and Glu residues were assumed to be charged, except Glu-153, 440, and 231D (when discussing residues, a letter "D" after the residue number

indicates that it belongs to that subunit; if no letter is given, it belongs to subunit C; subunits A and B are identical to the C and D residues, respectively, and therefore not explicitly discussed). Cys residues coordinating to Fe ions were assumed to be deprotonated, whereas the His residue that coordinates to Mo was protonated on the NE2 atom (we denote atoms by their PDB names). A thorough manual investigation of all the other His residues gave the following assignment:[28] His-274, 451, 297D, 359D and 519D were assumed to be protonated on the ND1 atom, His-31, 196, 285, 383, 90D, 185D, 363D and 457D were presumed to be protonated on both the ND1 and NE2 atoms (and therefore positively charged), whereas the remaining 14 His residues were modelled with a proton on the NE2 atom. Residues His-31, 363D and 429D were flipped (i.e. the C and N atoms in the imidazole ring were exchanged). Protons were added by the Maestro software,[30] optimising the hydrogen-bond network. The homocitrate was modelled in the singly protonated state with a proton shared between the hydroxyl group (which coordinates to Mo) and the O1 carboxylate atom. This protonation state was found to be most stable in a recent extensive QM/MM, molecular dynamics and quantum-refinement study.[28] In that study, the protonation states of His-195, 274, 362, 451, Glu-153, 380, 440 and Asp-443 were also confirmed by molecular dynamics simulations. The single protonation of the alcoholic group of homocitrate is also supported by another recent study.[31]

QM calculations

All QM calculations were performed with the Turbomole software (version 7.1).[32] We employed two DFT methods, TPSS[33] and B3LYP,[34–36] and two different basis sets of increasing size, def2-SV(P)[37] and def2-TZVPD.[38] The calculations were sped up by expanding the Coulomb interactions in an auxiliary basis set, the resolution-of-identity (RI) approximation.[39,40] Empirical dispersion corrections were included with the DFT-D3 approach[41] and Becke–Johnson damping,[42] as implemented in Turbomole.

The FeMo cluster was modelled by $MoFe_7S_9C$(homocitrate)(CH_3S)(imidazole) (53 atoms), where the two last groups are models of Cys-275 and His-442 (show in Figure 1). Following recent Mössbauer, anomalous dispersion and QM investigations,[11,16,31,43] we used the oxidation state-assignment $Mo^{III}Fe_3^{II}Fe_4^{III}$ of the metal ions in the resting state, giving a net charge of –5 for the QM system. We also studied the states with an extra electron (called the reduced state) and with an extra proton (called the protonated state). After a thorough investigation of over 50 different positions for the added proton in the BS7 state, protonation of the S2B atom (the names of the atoms follow those in the crystal structure and are shown in Figure 1a) was found to be most stable.[44] This atom forms a hydrogen bond to His-195, which has been suggested to deliver protons to the cluster.[3,16] In these calculations, the QM system was enhanced with models of Arg-96, His-195 and Arg-359 (sidechains), Ile-355, Gly-356 (backbone), as well as two water molecules, because they form hydrogen bonds to the FeMo cluster, in total 114 atoms (net charge –2; shown in Figure 1b).[44] The resting and protonated states were modelled either in the quartet spin state with a surplus of three α electrons (which is the experimental ground state[3,11]) or the doublet state. For the reduced state, we tested the (open-shell) singlet, triplet and quintet states (the latter is the experimental ground state[45]).

The electronic structure was obtained with the BS approach.[20] In practice, this means that each of the seven Fe ions were modelled in the high-spin state, with either a surplus of α (four Fe ions) or β (three Fe ions) spin. Such a state can be selected in 35 different ways ($\frac{7!}{3!\,4!}$). All of these were studied individually. A starting wavefunction was obtained by first optimising the all-high-spin state with 35 unpaired electrons and then changing the total α and β occupation numbers to the desired net spin. This gave one of the BS states. The other BS

states were obtained by simply swapping the coordinates of the Fe ions.[46] In some cases, we instead had to use the fragment approach by Szilagyi and Winslow to obtain a proper starting state.[47]

MM calculations

All MM calculations were performed with the Amber software.[48] For the protein, we used the Amber ff14SB force field[49] and water molecules were described by the TIP3P model.[50] For the metal sites, the MM parameters and charges were the same as in our previous investigation:[28] They were treated by a non-bonded model and metal sites outside the QM system were kept at the crystal-structure geometry.

The protein was solvated in a sphere with a radius of 70 Å around the geometrical centre of the protein. 160 Cl^- and 182 Na^+ ions were added at random positions outside the protein[28] to neutralise the protein and give an ionic strength of 0.2 M.[51] The final system contained 133 915 atoms. The added protons, counter ions and water molecules were optimised by a simulated annealing calculation (up to 370 K), followed by a minimisation, keeping the other atoms fixed at the crystal-structure positions.[28]

QM/MM calculations

The QM/MM calculations were performed with the ComQum software.[52,53] In this approach, the protein and solvent are split into two subsystems: System 1 (the QM region) was relaxed by QM methods, whereas system 2 contained the remaining part of the protein and the solvent. It was kept fixed at the original coordinates (equilibrated crystal structure).

In the QM calculations, system 1 was represented by a wavefunction, whereas all the other atoms were represented by an array of partial point charges, one for each atom, taken from the MM setup. Thereby, the polarisation of the QM system by the surroundings is included in a self-consistent manner (electrostatic embedding). When there is a bond between systems 1 and 2 (a junction), the hydrogen link-atom approach was employed: The QM system was capped with hydrogen atoms (hydrogen link atoms, HL), the positions of which are linearly related to the corresponding carbon atoms (carbon link atoms, CL) in the full system.[52,54] All atoms were included in the point-charge model, except the CL atoms.[55]

The total QM/MM energy in ComQum was calculated as[52,53]

$$E_{\mathrm{QM/MM}} = E^{\mathrm{HL}}_{\mathrm{QM1+ptch2}} + E^{\mathrm{CL}}_{\mathrm{MM12},q_1=0} - E^{\mathrm{HL}}_{\mathrm{MM1},q_1=0} \quad (3)$$

where $E^{\mathrm{HL}}_{\mathrm{QM1+ptch2}}$ is the QM energy of the QM system truncated by HL atoms and embedded in the set of point charges modelling system 2 (but excluding the self-energy of the point charges). $E^{\mathrm{HL}}_{\mathrm{MM1,q1=0}}$ is the MM energy of the QM system, still truncated by HL atoms, but without any electrostatic interactions. Finally, $E^{\mathrm{CL}}_{\mathrm{MM12,q1=0}}$ is the classical energy of all atoms in the system with CL atoms and with the charges of the QM region set to zero (to avoid double counting of the electrostatic interactions). Thus, ComQum employs a subtractive scheme with electrostatic embedding and van der Waals link-atom corrections.[56] By this approach, some errors caused by the truncation of the QM system should cancel.

The geometry optimisations were continued until the energy change between two iterations was less than 2.6 J/mol (10^{-6} a.u.) and the maximum norm of the Cartesian gradients was below 10^{-3} a.u. The QM/MM geometry optimisations were performed using the TPSS-D3 method[33,41] and the def2-SV(P)[37] basis set. Single-point QM/MM energy calculations were then performed at the TPSS-D3/def2-TZVPD and B3LYP-D3/def2-TZVPD levels of theory.

Result and Discussion

In this paper, we have performed a thorough systematic study of the BS states of the FeMo cluster in nitrogenase with QM/MM methods with the aim of developing a practical procedure to deal with the large number of possible states for each intermediate in the reaction mechanism. We study the resting $Mo^{III}Fe_3^{II}Fe_4^{III}$ state, as well as the one-electron reduced $Mo^{III}Fe_4^{II}Fe_3^{III}$ state, and the resting state with an extra proton on the S2B atom. The structures of the resting and the protonated states are shown in Figures 1a and 1b, respectively. Previous studies have shown that the seven Fe ions in the FeMo cluster all reside in their high-spin states,[20] whereas the Mo ion is in the unusual intermediate-spin Mo(III) state with one unpaired electron.[11] Therefore, to reach the experimentally observed quartet state (with a surplus of three α electrons), four of the Fe ions need to have the dominant α spin and three should have the opposite β spin. In the asymmetric protein, this can be selected in 35 ($\frac{7!}{3!\,4!}$) different ways. Employing the approximate C_3 symmetry of the cluster, they can be grouped in 10 BS states, defined by Noodleman[20] and shown in Figure 2. We have systematically studied all these 35 BS states in the two or three lowest spin states and investigated how their relative energies depend on the DFT method, the basis set, the surroundings and the geometry. The results for the resting, reduced and protonated states are described in separate sections.

Resting state

Figure 3a shows the relative energies of the 35 BS states for the resting state in the quartet spin state, obtained at the TPSS-D3/def2-SV(P) level of theory after QM/MM geometry optimisation. It can be seen that the energies of the 35 states vary by 117 kJ/mol. Three states are lowest in energy and they represent the three variants of Noodleman's BS7 state in the asymmetric protein. Their QM/MM energies differ by only 2 kJ/mol, i.e. less than in the previous studies in vacuum and in a Poisson–Boltzmann model of the protein.[20,27] Next, come the three BS6 states, which are ~27 kJ/mol less stable. The three states again have energies that agree within 2 kJ/mol. They are followed by the single BS2 state, which is only 3–5 kJ/mol less stable. The other states come in the order BS8 < BS4 ≈ BS10 < BS9 < BS5 < BS3 < BS1.

The difference in energies comes mainly from the QM energy term ($E^{\mathrm{HL}}_{\mathrm{QM1+ptch2}}$ in Eqn. 3): The MM contribution ($E^{\mathrm{CL}}_{\mathrm{MM12},q_1=0} - E^{\mathrm{HL}}_{\mathrm{MM1},q_1=0}$ in Eqn. 3) varies by only 8 kJ/mol among the 35 states, with a less clear variation among the various states (most favourable for some BS3, BS4 and BS5 states; least favourable for the BS9 and BS10 states). The influence of the electrostatics of the surroundings (i.e. the difference in the relative energies for $E^{\mathrm{HL}}_{\mathrm{QM1+ptch2}}$ and for the QM energy without the point-charge model) is also minor, affecting the relative energies by up to 10 kJ/mol (3 kJ/mol on average).

The optimised structure of the FeMo cluster in the best BS7 state closely resembles that in the crystal structure of the nitrogenase,[6] as can be seen in Figure 4. The root-mean-squared deviation (RMSD) is only 0.06 Å. The other two BS7 structures give similar results (RMSD = 0.07 Å), but also the best BS6 and BS10 states have the same RMSD, whereas that of the (least favourable) BS1 state is 0.10 Å. Comparing the 15 short (< 3.0 Å) Mo–Fe and Fe–Fe distances gives a mean absolute deviation (MAD) of 0.05 Å for all three BS7 states and also for the best BS6 state, whereas that of the best BS10 state and BS1 were 0.04 and 0.07 Å, respectively. The maximum deviation is 0.09 Å for all BS7 states and also for BS10, whereas it is 0.16 Å for BS6 and 0.20 Å for BS1. This shows that the QM/MM optimisations give excellent structures and that the BS7 states reproduce the crystal structure excellently. Similar results were obtained in a recent study (slightly larger RMSD, e.g. 0.10 Å for the best BS7

state, but smaller deviations of the Fe–Fe and Mo–Fe distances, e.g. a MAD of only 0.02 Å for the best BS7 state).[24]

Geometry optimisations of the FeMo cluster in the various BS states are quite time-consuming, often requiring hundreds of iterations. Single-point energy calculations are much faster (1–3 hours on a single processor at the TPSS/def2-SV(P) level, when started from another BS state). Therefore, it is of great interest to see how reliable BS-state energies without geometry optimisation are. Such energies are shown in Figure 3b (single-point calculations on the optimised structure of the BS7-1 state). The effect of the geometry optimisation is relatively small for most states, with an average of 13 kJ/mol and a maximum value of 37 kJ/mol. As expected, all energy differences increase, with the smallest differences for the BS7 (0–3 kJ/mol) and BS8 states (2–8 kJ/mol) and the largest differences for the BS1 (37 kJ/mol) state. There is a nearly perfect correlation between the relative energies of the BS state obtained with or without geometry optimisation, $R^2 = 0.98$, but the slope is 1.3, showing that the least stable states are most affected by the geometry optimisation. Still, the accuracy is enough to rapidly discard most BS states.

Figure 3c shows the relative energies of the 35 BS states calculated by single-point energy calculations at the TPSS-D3/def2-TZVPD level of theory, i.e. with an appreciably larger basis set (at the geometry optimised for each state with TPSS/def2-SV(P)). It can be seen that the ordering of the states is quite similar to that obtained with the smaller basis set, with a correlation of $R^2 = 0.97$ between the two sets of energies. The change in the relative energies of the various BS states is in general small, less than 9 kJ/mol, with a signed average of only 1 kJ/mol (unsigned average of 4 kJ/mol), but for BS1, it is 20 kJ/mol.

Changing the QM method to the hybrid B3LYP-D3 functional (still with the large def2-TZVPD basis set and the same geometry) has an appreciably larger effect on the relative BS energies, as can be seen in Figure 3d. They change by up to 54 kJ/mol (125 kJ/mol for the BS1 state), with an unsigned average of 27 kJ/mol. The correlation between the TPSS and B3LYP relative energies (with the same basis set) is $R^2 = 0.68$. The BS7 states are still most stable, but they show a slightly larger variation of 6 kJ/mol and the BS7-3 state is now most stable. However, the BS2 and BS6 states are strongly destabilised by B3LYP, 66 and 49–52 kJ/mol less stable than the BS7-3 state. Instead, the BS10 states, become the second most stable, 12–21 kJ/mol less stable than BS7-3, followed by BS8 (20–29 kJ/mol less stable than BS7-3).

The spin distribution is quite similar for the 35 BS states (shown in Table S2). With the def2-SV(P) basis set, the seven Fe ion have a spin populations of 2.2–3.3 for most states. The Mo ion shows a larger variation among the BS states: For most states, it is rather low, 0.2–0.4 (positive for the BS4–BS6 states and negative for the BS7–BS10 states). However, for BS1, BS2 and BS3 it is instead ±0.9. The spin on the central C atom is small, up to 0.2 and in general negative, except for the BS2, BS7 and BS8 states. The Cys ligand also has a small spin density, up to 0.1, zero or negative for most states, except for the same three BS states as for the C atom. The His and HCA ligands always have negligible spin (<0.01). The spin on the sulfide ions is larger, up to 0.35, with a varying sign. Most S^{2-} ions have a small spin, up to 0.12. However, the three μ_2 bridging S^{2-} ions (S2B, S3A and S55A) quite often have a spin of 0.2–0.35.

The TPSS/def2-TZVPD calculations give similar spin densities, with mean absolute differences of 0.1. The spin on Fe ions is often slightly smaller, and that on the Mo and S^{2-} ions slightly higher. On the other hand, the spin densities in the B3LYP calculations are more different, with mean absolute differences of 0.4 for Mo, 0.6 for Fe, but only 0.04 for S. The spin on Mo is larger, 0.6–0.8 for most BS states (positive or negative), but –1.9 to –2.1 for BS2 and BS3. The Fe spin populations are also somewhat larger, 3.1–3.6 in all low-energy BS states.

We have studied the 35 BS states also in the doublet state for the resting state. The results are presented in Figure 5 (energies relative to the best quartet BS7-1 state). As for the quartet state, the effect of the basis set was quite small (less than 11 kJ/mol); therefore, we will only discuss the results with the larger basis set. Interestingly, the doublet was lower in energy than the quartet for most BS states with the TPSS method, by 2–31 kJ/mol. However, for the BS7 states, the opposite is true by 40–42 kJ/mol. The quartet is lower in energy also for the BS4, BS6 and BS8 states, but only by 0–19 kJ/mol. As a consequence, the BS10 states are lowest in energy for the doublet, 15–20 kJ/mol lower than the best BS7 state. However, they are still at least 20 kJ/mol less stable than the best (BS7) quartet state.

In contrast, all doublet states are disfavoured by the B3LYP functional (which is known to favour high-spin states), by 7–82 kJ/mol. The effect is smallest for the BS2 state and largest for the BS6 and BS8 states. For the BS7 states, the effect is ~34 kJ/mol. The BS10 states, are disfavoured by 47–55 kJ/mol, which makes them the most stable doublet states. However, they are still at least 55 kJ/mol less stable than the best quartet state.

The spin densities of the doublet states are quite similar to those of the quartet states: Those of the Mo ion differ by only 0.13 on average, but in some cases, the difference is significant. For example, the Mo spin is reduced from –0.3 to nearly zero for the BS8 states. The difference in spin of the C^{4-} and S^{2-} ions are also small, 0.03 and 0.07 on average. The change for the Fe ions is larger, 0.36 on average, reflecting the change in total spin by two electrons, but typically only two or three Fe ions show a large change (0.3–2.2). For most BS states (not BS9 and BS10), one Fe ion has a low spin density of 1.1–1.9 (0.5 for BS1). For BS2–BS6, only a single (none for BS1) Fe ion has a spin larger than 3.0.

Reduced states

We have also studied the one-electron reduced states, to get an impression how the relative stabilities of the various BS states change when the FeMo cluster is reduced. Adding an electron to the quartet resting state with a surplus of three α electrons would give either a quintet state (if the added electron is of α spin) or a triplet state (if the added electron is of β spin) and both these states were studied. We also studied the open-shell singlet state, because some previous studies have assumed that all reduced states have the lowest possible spin state.[16]

We first discuss the quintet state. Figure 6a shows in blue the TPSS/def2-SV(P) energies for all states, obtained with QM/MM optimised geometries. It can be seen that they are quite similar to those obtained for the resting state (cf. Figure 3a). The energies vary by 88 kJ/mol. BS7 is lowest in energy, 21–32 kJ/mol lower than the BS4, BS6 and BS8 states, which all are close in energy.

When using a fixed geometry (that of the BS7-1 resting state), all the other states are destabilised by 3–46 kJ/mol (20 kJ/mol on average). The other two BS7 states are destabilised by 12–14 kJ/mol, which is larger than for the resting state. The correlation to the energies after optimisation is good ($R^2 = 0.93$), although slightly worse than for the resting state, probably because the starting geometry was that of the resting state, not the BS7 geometry of the reduced state.

Changing the basis set to def2-TZVPD has a quite small effect on the relative energies, 0–11 kJ/mol, except for BS1 (45 kJ/mol), increasing all energy differences. The correlation to the energies obtained with the smaller basis set is 0.94.

Changing to the B3LYP method has a somewhat larger effect on the energies (15 kJ/mol on average), giving a correlation of $R^2 = 0.72$ to the TPSS energies. The relative energies of all states increase, except for the BS9 and BS10 states, which are stabilised by 3–7 and 14–26 kJ/mol, respectively. Consequently, BS7 is still the most stable state, but BS10 is the second

best (21–27 kJ/mol less stable). The BS2, BS3 and BS6 states are strongly destabilised.

Compared to the resting state, the relative energies of the various spin states change by up to 43 kJ/mol. At the TPSS level, most states are stabilised relative to the BS7 state, in particular BS3 and BS5 (by 12–32 kJ/mol). At the B3LYP level, effects are somewhat larger (MAD = 14 kJ/mol) and with more varying signs. The BS5, BS9 and BS10 states are stabilised by up to 28 kJ/mol, whereas the others are destabilised.

The spin densities (Table S3) are quite similar to those of the resting states: Those on Mo, C and S agree to within 0.2, 0.1 and 0.3 for all BS states, respectively. On the other hand, the Fe spin densities may differ by up to 0.8, reflecting the extra electron (and spin) for the reduced states, although the average difference is only 0.3.

The triplet spin state is slightly less stable than the quintet state at all levels of theory, as can be seen in Figure 6b. The energy difference between the best triplet and quintet states is 14, 16 and 19 kJ/mol for the TPSS/def2-SV(P), TPSS/def2-TZVPD and B3LYP/def2-TZVPD calculations, respectively. The most interesting difference compared to the quintet state is that with the TPSS functional, the BS2, BS6, BS7 and BS10 states have the same energy within 10 kJ/mol, actually with BS10-5 and BS2 lowest (2 kJ/mol lower than BS7-1). However, at the B3LYP level of theory, BS10 is somewhat destabilised and BS2 is considerably destabilised, so that BS7-3 becomes the most stable state by at least 10 kJ/mol before the BS10 and BS8 states.

With the TPSS functional, most states are more stable in the triplet than in the quintet state, in particular the BS1, BS2 and BS10 states (by 21–48 kJ/mol). However, the BS7 states are 16–23 kJ/mol more stable in the quintet state. In contrast, at the B3LYP level, only the BS2, BS3 and BS8 states are more stable in the triplet state, by 3, 39–48 and 2–12 kJ/mol, respectively. For the BS1, BS4, BS5, BS6 and BS7 states, the quintet is appreciably more stable, by 132, 26–33, 33–67, 12–26, and 18–21 kJ/mol, respectively.

The spin densities of the triplet states are quite similar to those of the quintet states, with average differences of 0.12 for Mo and 0.03 for the C^{4-} and S^{2-} ions. For the Fe ions, the differences are larger, 0.4 on average, reflecting the reduction of the total spin by 2. In general, one or two Fe ions have a lower spin (1.6–2.5, but 0.2 for BS1) than the other ions.

The open-shell singlet state has a similar stability as the triplet state, as can be seen in Figure 6c: It is 23, 16 and 35 kJ/mol less stable than the quintet state at the TPSS/def2-SV(P), TPSS/def2-TZVPD and B3LYP/def2-TZVPD levels of theory, respectively. With the TPSS functional, the BS2, BS6 and BS10 states are actually more stable than the BS7 states (for the singlets), by 2–14 kJ/mol. The basis-set effect is also unusually large, up to 24 kJ/mol for the BS3 states. With the B3LYP functional, the singlet state is disfavoured for most BS states, except BS2 and BS3, so that these states become most stable (50–60 kJ/mol more stable than the best BS7 state). However, they are still 35–45 kJ/mol less stable than the best (BS7-1) quintet state.

The spin densities of the singlet states are still quite similar to those of the quintet states, with average differences of 0.19, 0.03 and 0.05 for Mo, C^{4-} and S^{2}. For the Fe ions, the differences are larger, 0.75 on average, reflecting the reduction of the total spin by 4. All BS states except BS3 have one (BS9 and BS10) or two Fe ions with a low spin (below 2).

Protonated states

Finally, we have studied the resting state with one added proton, to investigate how the BS-state preferences change when the FeMo cluster is protonated. These calculations were performed on a larger QM model, including all groups forming hydrogen bonds to the FeMo cluster (Figure 1b). Based on a thorough study of more than 50 potential protonation sites (for the BS7-1 state at the TPSS/def2-TZVPD level), it was found that it is most favourable to

protonate the bridging S2B atom (Figure 1).[44] Protonation of this atom led to somewhat elongated Fe–S2B bonds (2.29–2.37 Å, compared to 2.18–2.19 Å in the resting state).

Relative energies of the various BS states of this protonated cluster are shown in Figure 7. It can be seen that at the TPSS/def2-SV(P) level of theory, the BS7 states still are the most stable, by 21–34 kJ/mol before the BS6 states. The effect of the basis set is still restricted, up to 11 kJ/mol, so the BS7 states remain most stable by 21–41 kJ/mol. The correlation (R^2) between the results with the two basis sets is 0.97. Single-point calculations on the BS7-1 structure of the protonated state gave similar energies with a correlation of 0.95.

As usual, B3LYP had a larger effect on the relative energies, favouring the BS8, BS9 and BS10 states (by up to 58 kJ/mol) and disfavouring the other states (by up to 53 kJ/mol, but 177 kJ/mol for BS1). As a consequence, the BS10 states gain a stability similar to that of BS7 states, with two states within 2 kJ/mol of the most stable BS7 state. The correlation to the TPSS results is 0.71.

Compared to the resting quartet state, the relative energies of the various BS states change by 8 (TPSS) or 12 kJ/mol (B3LYP) on average. The largest changes are observed for the BS1 and BS10 states with B3LYP (up to 33 kJ/mol). Compared to the reduced quintet state, the differences are larger, 14–23 kJ/mol on average, with the largest effect (up to 59 kJ/mol) for the BS5 states with both functionals. This shows that protonation and enlarging the QM model have a smaller effect on the BS energies than reducing the cluster.

The spin densities (Table S4) are quite similar to those of the resting states: Those of the Mo, C and S ions change by 0.07, 0.01 and 0.07 on average, respectively. The spin on the Fe ions change more, by 0.3 on average, but not in any systematic way.

We also studied the 35 BS states of the doublet state, as is shown in Figure 8. However, it was found to always be at least 16 kJ/mol less stable than the quartet state at the TPSS/def2-SV(P) level of theory and by 61 kJ/mol at the B3LYP/def2-SV(P) level of theory. These results are quite similar to those obtained for the resting state.

Finally, we studied also another protonation state, with a proton on the S2A atom (a μ_3 S^{2-} ion on the Cys-275 side of the cluster) instead on the S2B atom. The structure is shown in Figure 9, where it can be seen that protonation of the S2A atom led to a large increase in the Fe1–S2A distance (from 2.25 Å in the resting state to 2.88 Å) and smaller increases in the other two Fe–S2A distances (from 2.27–2.29 Å to 2.32–2.38 Å). The structures were either optimised for each BS state individually or for the BS7-3 state for both protonation states with the energy difference calculated by single-point energy calculations for each of the 35 BS states (same state for both protonation states). The spin-state ordering is shown in Figure 10 and it can be seen that they are quite similar to those of the structures protonated on S2B, shown in Figure 7. Even more importantly, all calculations indicated that it was more favourable to have the proton on the S2B atom than on the S2A atom. The energy difference was also rather consistent, 26–58 kJ/mol (33 kJ/mol for BS7-3, but ~85 kJ/mol for BS2). These calculations show that the BS states do not change the relative energy of the various protonation states by more than 32 kJ/mol.

Conclusions

In this paper, we have performed a thorough and systematic study of the BS states of the FeMo cluster in nitrogenase. Structures of all 35 BS states were optimised with QM/MM inside the protein using the TPSS-D3/def2-SV(P) method. More accurate energies were calculated with the larger def2-TZVPD basis set and the B3LYP method. We have studied three states of the FeMo cluster, the resting state, the one-electron reduced state and a protonated state with a proton on the S2B or S2A atoms. The calculations are intended to give an indication of how future studies of this large cluster with its complicated spin coupling

should be performed. We have obtained many useful results.

- The effect of the basis set is quite small, changing the relative energies of the BS states by less than 11 kJ/mol (occasionally more for the BS1 state, which always is high in energy) when going from def2-SV(P) to def2-TZVPD. Moreover, the correlation (R^2) between the results obtained with the two basis sets is always good, 0.92–0.97. Therefore, initial evaluation of structures and spin states can be performed with a split-valence basis set.
- Single-point calculations on one geometry also give good correlations to results obtained with optimised structures, 0.92–0.98. However, the effect on energies is larger, up to 37 kJ/mol (46 kJ/mol if structures of another oxidation state are used). Thus, a first scan of the energies of the various BS states can be performed without optimising the geometries, but it must be remembered that this will favour the BS state, for which the geometry was obtained.
- The DFT functional has a quite large effect on the relative energies of the various spin and BS states. As expected, the hybrid functional favours higher spin states, but the effect is not uniform for all BS states. TPSS and B3LYP give relative energies of the BS states that may differ by up to 58 kJ/mol and the correlation is rather poor, 0.57–0.72. Therefore, both a pure and a hybrid functional should be used to decide which BS state is most stable.
- For all three states studied (resting, reduced and protonated states), BS7 was found to be most stable with both functionals, and they also both predicted that the most stable spin state was as the quartet for the resting state and the quintet for the reduced state, in accordance with experimental results.[3,45] The second most stable BS state was BS6 for TPSS and BS10 for B3LYP. The energy difference was 21–26 and 12–22 kJ/mol, respectively. Only for the protonated state with B3LYP was the assignment of the ground state ambiguous, because the BS7 and BS10 states were essentially degenerate.
- The 3–6 BS states of the same C_3-symmetry type (shown in Figure 2) had similar energies, within 14 kJ/mol. Thus, the protein has a rather small influence on the relative energies of the BS states related by the approximate three-fold symmetry of the FeMo cluster. This means that for initial investigations, it is enough to study only one example of each of the 10 symmetry-distinct BS states. In particular, the most stable of the three BS7 states varied in the various calculations. Thus, we do not find any preference for any of the three BS7 states in the protein.

Based on these results, we suggest the following procedure for the study of the reaction mechanism of nitrogenase: For each new protonation or oxidation state, possible conformations or protonations should be studied with DFT and medium-sized basis sets (e.g. TPSS-D3/def2-SV(P)), using the BS and spin state expected to be best (i.e. the one that was most stable for the previous state). For the best structures, check the energies of the various BS states and other possible spin multiplicities. This can be done without geometry optimisation, with the same basis set and only for the 10 symmetry distinct BS states, but both a pure and a hybrid functional should be used. If several BS states are degenerate within ~20 kJ/mol, geometry optimisation and calculations with larger basis sets are needed. If a different BS or spin state is found to be most stable, the procedure needs to be repeated. If the two DFT functionals give differing results regarding the most stable BS state, both states need to be examined and the energy difference indicate the uncertainty in the calculations. Finally, an accurate energy should be calculated with a large basis set and it can be determined which of the 3 or 6 non-symmetric BS states is most stable.

The present study gave the correct quartet ground state for the resting state of the FeMo cluster[3] and excellent structures compared to the crystal structure (Figure 4),[6] providing

credence to the approach. On the other hand, the calculations do not support previous suggestions that all intermediates should have the lowest possible spin multiplicity.[16] On the contrary, we find the higher multiplicities more stable, in accordance with the results of Kästner and Blöchl.[26] That study also suggested that all intermediates are in the BS7 or BS6 states. This is in agreement with our results with the TPSS functional, showing that these two states are lowest for all three complexes studied. However, our results indicate that this conclusion may change if a hybrid functional is used instead.

The fact that different DFT functionals give differing results (by up to 58 kJ/mol) is of course problematic. Unfortunately, there is currently no ab initio QM method that can be used to calibrate the DFT calculations, although several groups work in this direction.[57–61] Therefore, the best that can be done is to compare results of several DFT methods; if they agree, the results can probably be trusted, whereas if they disagree, the difference reflects the uncertainty in the calculations. Our and others experience indicate that calculations with a pure and a hybrid functional or with two hybrid functionals with different amounts of Hartree–Fock exchange give a fast indication whether the results depend on the functional.[62,63]

Acknowledgements

This investigation has been supported by grants from the Swedish research council (project 2014-5540), from COST through Action CM1305 (ECOSTBio) and by a scholarship to LC from the China Scholarship Council. The computations were performed on computer resources provided by the Swedish National Infrastructure for Computing (SNIC) at Lunarc at Lund University and HPC2N at Umeå University.

References

(1) Burgess, B. K.; Lowe, D. J. *Chem. Rev.* **1996**, *96* (7), 2983–3012.
(2) Schmid, B.; Chiu, H.-J.; Ramakrishnan, V.; Howard, J. B.; Rees, D. C. In *Handbook of Metalloproteins*; John Wiley & Sons, Ltd, 2006; pp 1025–1036.
(3) Hoffman, B. M.; Lukoyanov, D.; Yang, Z.-Y.; Dean, D. R.; Seefeldt, L. C. *Chem. Rev.* **2014**, *114* (8), 4041–4062.
(4) Kim, J.; Rees, D. C. *Science (80-.).* **1992**, *257* (5077), 1677–1682.
(5) Einsle, O.; Tezcan, F. A.; Andrade, S. L. A.; Schmid, B.; Yoshida, M.; Howard, J. B.; Rees, D. C. *Science (80-.).* **2002**, *297* (5587), 1696.
(6) Spatzal, T.; Aksoyoglu, M.; Zhang, L.; Andrade, S. L. A.; Schleicher, E.; Weber, S.; Rees, D. C.; Einsle, O. *Science (80-.).* **2011**, *334* (November), 940–940.
(7) Spatzal, T.; Perez, K. A.; Einsle, O.; Howard, J. B.; Rees, D. C. *Science (80-.).* **2014**, *345* (6204), 1620–1623.
(8) Einsle, O. *J. Biol. Inorg. Chem.* **2014**, *19* (6), 737–745.
(9) Eady, R. R. *Chem. Rev.* **1996**, *96* (7), 3013–3030.
(10) Lancaster, K. M.; Roemelt, M.; Ettenhuber, P.; Hu, Y.; Ribbe, M. W.; Neese, F.; Bergmann, U.; DeBeer, S. *Science (80-.).* **2011**, *334* (6058), 974–977.
(11) Bjornsson, R.; Lima, F. A.; Spatzal, T.; Weyhermüller, T.; Glatzel, P.; Bill, E.; Einsle, O.; Neese, F.; DeBeer, S. *Chem. Sci.* **2014**, *5* (8), 3096–3103.
(12) Thorneley, R. N. F.; Lowe, D. J. In *Molybdenum Enzymes*; Spiro, T. G., Ed.; Wiley: New York, 1985; pp 221–284.
(13) Tuczek, F. In *RSC Metallobiology Series 7*; Hille, R., Schulzke, C., Kirk, M. L., Eds.; Royal Society of Chemistry: Cambridge, 2017; pp 223–274.
(14) Dance, I. *Zeitschrift für Anorg. und Allg. Chemie* **2015**, *641*, 91–99.

(15) Varley, J. B.; Wang, Y.; Chan, K.; Studt, F.; Nørskov, J. K. *Phys. Chem. Chem. Phys.* **2015**, *17* (44), 29541–29547.
(16) Siegbahn, P. E. M. *J. Am. Chem. Soc.* **2016**, *138* (33), 10485–10495.
(17) McKee, M. L. *J. Phys. Chem. A* **2016**, *120* (5), 754–764.
(18) Rao, L.; Xu, X.; Adamo, C. *ACS Catal.* **2016**, *6* (3), 1567–1577.
(19) Dance, I. *J. Inorg. Biochem.* **2017**, *169*, 32–43.
(20) Lovell, T.; Li, J.; Liu, T.; Case, D. A.; Noodleman, L. *J. Am. Chem. Soc.* **2001**, *123*, 12392–12410.
(21) Lukoyanov, D.; Pelmenschikov, V.; Maeser, N.; Laryukhin, M.; Yang, T. C.; Noodleman, L.; Dean, D. R.; Case, D. A.; Seefeldt, L. C.; Hoffman, B. M. *Inorg. Chem.* **2007**, *46* (26), 11437–11449.
(22) Dance, I. *Inorg. Chem.* **2011**, *50* (1), 178–192.
(23) Harris, T. V; Szilagyi, R. K. *Inorg. Chem* **2011**, *50*, 4811–4824.
(24) Benediktsson, B.; Bjornsson, R. *Inorg. Chem.* **2017**, *56*, 13417–13429.
(25) Xie, H.; Wu, R.; Zhou, Z.; Cao, Z. *J. Phys. Chem. B* **2008**, *112* (36), 11435–11439.
(26) Kästner, J.; Blöchl, P. E. *J. Am. Chem. Soc.* **2007**, *129*, 2998–3006.
(27) Lovell, T.; Li, J.; Case, D. A.; Noodleman, L. *J. Biol. Inorg. Chem.* **2002**, *7* (7–8), 735–749.
(28) Cao, L.; Caldararu, O.; Ryde, U. *J. Phys. Chem. B* **2017**, *121*, 8242–8262.
(29) Olsson, M. H. M.; Søndergaard, C. R.; Rostkowski, M.; Jensen, J. H. *J. Chem. Theory Comput.* **2011**, *7* (2), 525–537.
(30) Schrödinger, L. Schrödinger, LLC: New York, NY 2016.
(31) Bjornsson, R.; Neese, F.; DeBeer, S. *Inorg. Chem.* **2017**, *56* (3), 1470–1477.
(32) Furche, F.; Ahlrichs, R.; Hättig, C.; Klopper, W.; Sierka, M.; Weigend, F. *Wiley Interdiscip. Rev. Comput. Mol. Sci.* **2014**, *4* (2), 91–100.
(33) Tao, J.; Perdew, J. P.; Staroverov, V. N.; Scuseria, G. E. *Phys. Rev. Lett.* **2003**, *91* (14), 146401.
(34) Becke, A. D. *Phys. Rev. A* **1988**, *38* (6), 3098–3100.
(35) Lee, C.; Yang, W.; Parr, R. G. *Phys. Rev. B* **1988**, *37* (2), 785–789.
(36) Becke, A. D. *J. Chem. Phys.* **1993**, *98* (2), 1372.
(37) Schäfer, A.; Horn, H.; Ahlrichs, R. *J. Chem. Phys.* **1992**, *97* (4), 2571–2577.
(38) Weigend, F.; Ahlrichs, R. *Phys. Chem. Chem. Phys.* **2005**, *7* (18), 3297–3305.
(39) Eichkorn, K.; Treutler, O.; Öhm, H.; Häser, M.; Ahlrichs, R. *Chem. Phys. Lett.* **1995**, *240* (4), 283–289.
(40) Eichkorn, K.; Weigend, F.; Treutler, O.; Ahlrichs, R. *Theor. Chem. Acc.* **1997**, *97* (1–4), 119–124.
(41) Grimme, S.; Antony, J.; Ehrlich, S.; Krieg, H. *J. Chem. Phys.* **2010**, *132* (15), 154104 (19 pages).
(42) Grimme, S.; Ehrlich, S.; Goerigk, L. *J. Comput. Chem.* **2011**, *32* (7), 1456–1465.
(43) Spatzal, T.; Schlesier, J.; Burger, E.-M.; Sippel, D.; Zhang, L.; Andrade, S. L. A.; Rees, D. C.; Einsle, O. *Nat. Commun.* **2016**, *7* (Iii), 10902.
(44) Cao, L.; Ryde, U. *J. Biol. Inorg. Chem.* **2017**, to be submitted.
(45) Yoo, S. J.; Angove, H. C.; Papaefthymiou, V.; Burgess, B. K. *J. Am. Chem. Soc.* **2000**, *122* (9), 4926–4936.
(46) Greco, C.; Fantucci, P.; Ryde, U.; Gioia, L. de. *Int. J. Quantum Chem.* **2011**, *111* (14), 3949–3960.
(47) Szilagyi, R. K.; Winslow, M. A. *J. Comput. Chem.* **2006**, *27* (12), 1385–1397.
(48) Case, D. A.; Berryman, J. T.; Betz, R. M.; Cerutti, D. S.; Cheatham, T. E.; Darden, T. A.; Duke, R. E.; Giese, T. J.; Gohlke, H.; Goetz, A. W.; Homeyer, N.; Izadi, S.; Janowski, P.; Kaus, J.; Kovalenko, A.; Lee, T. S.; LeGrand, S.; Li, P.; Luchko, T.; Luo,

R.; Madej, B.; Merz, K. M.; Monard, G.; Needham, P.; Nguyen, H.; Nguyen, H. T.; Omelyan, I.; Onufriev, A.; Roe, D. R.; Roitberg, A. E.; Salomon-Ferrer, R.; Simmerling, C.; Smith, W.; Swails, J.; Walker, R. C.; Wang, J.; Wolf, R. M.; Wu, X.; York, D. M.; Kollman, P. A. University of California: San Francisco 2014.

(49) Maier, J. A.; Martinez, C.; Kasavajhala, K.; Wickstrom, L.; Hauser, K. E.; Simmerling, C. *J. Chem. Theory Comput.* **2015**, *11*, 3696–3713.

(50) Jorgensen, W. L.; Chandrasekhar, J.; Madura, J. D.; Impey, R. W.; Klein, M. L. *J. Chem. Phys.* **1983**, *79* (2), 926–935.

(51) Barney, B. M.; Mcclead, J.; Lukoyanov, D.; Laryukhin, M.; Yang, T.; Dean, D. R.; Hoffman, B. M.; Seefeldt, L. C. *Biochemistry* **2007**, *46*, 6784–6794.

(52) Ryde, U. *J. Comput. Aided. Mol. Des.* **1996**, *10*, 153–164.

(53) Ryde, U.; Olsson, M. H. M. *Int. J. Quantum Chem.* **2001**, *81*, 335–347.

(54) Reuter, N.; Dejaegere, A.; Maigret, B.; Karplus, M. *J. Phys. Chem. A* **2000**, *104* (8), 1720–1735.

(55) Hu, L.; Söderhjelm, P.; Ryde, U. *J. Chem. Theory Comput.* **2011**, *7* (3), 761–777.

(56) Cao, L.; Ryde, U. *J. Chem. Theory Comput.* **2017**, *submitted*.

(57) Sharma, S.; Sivalingam, K.; Neese, F.; Kin-Lic, C. *Nat Chem* **2014**, *6* (10), 927–933.

(58) Delcey, M. G.; Pierloot, K.; Phung, Q. M.; Vancoillie, S.; Lindh, R.; Ryde, U. *Phys. Chem. Chem. Phys.* **2014**, *16* (17), 7927–7938.

(59) Dong, G.; Phung, Q. M.; Hallaert, S. D.; Pierloot, K.; Ryde, U. *Phys. Chem. Chem. Phys.* **2017**, *19*, 10590–10601.

(60) Freitag, L.; Knecht, S.; Angeli, C.; Reiher, M. *J. Chem. Theory Comput.* **2017**, *13* (2), 451–459.

(61) Reiher, M.; Wiebe, N.; Svore, K. M.; Wecker, D.; Troyer, M. *Proc. Natl. Acad. Sci.* **2017**, *114* (29), 7555–7560.

(62) Blomberg, M. R. A.; Borowski, T.; Himo, F.; Liao, R.-Z.; Siegbahn, P. E. M. *Chem. Rev.* **2014**, *114* (7), 3601–3658.

(63) Li, J.; Mata, R. A.; Ryde, U. *J. Chem. Theory Comput.* **2013**, *9* (3), 1799–1807.

Figure 1. The QM model used for the FeMo cluster of nitrogenase (a) in the resting and reduced state, showing also the names of the various atoms, and (b) the extended QM model used in the protonated state (note the extra proton on the S2B atom).

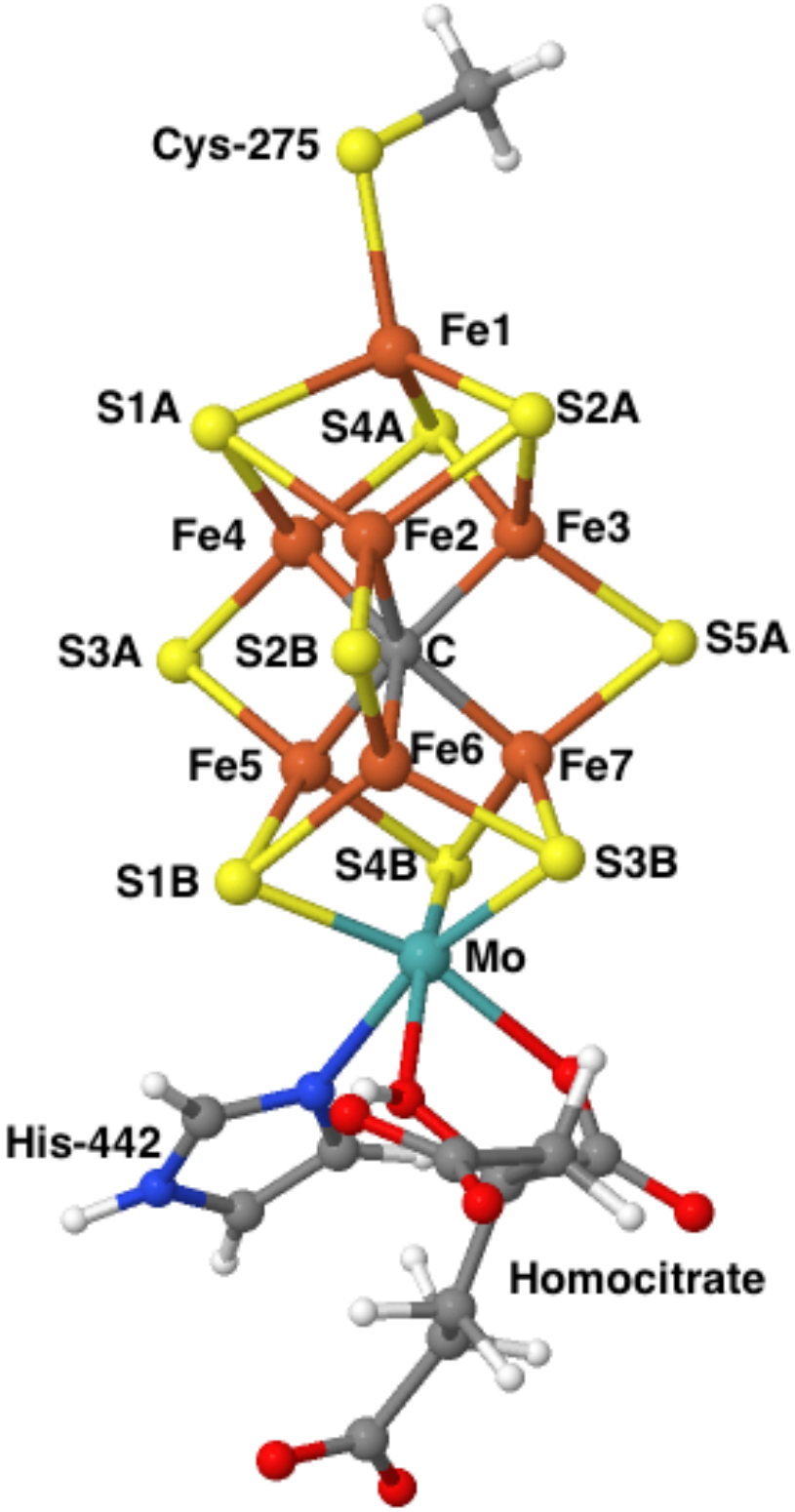

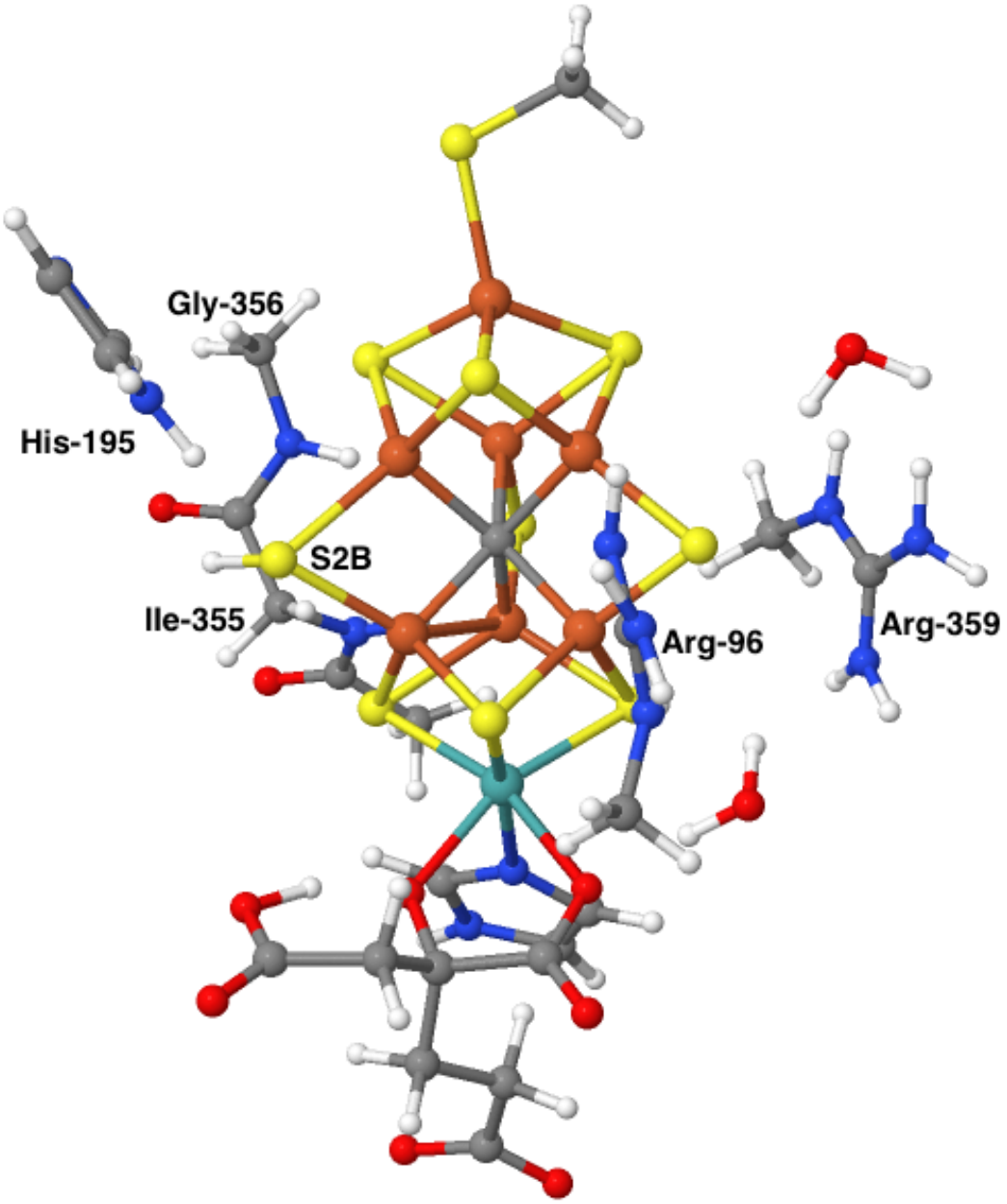
Gly-356
His-195
S2B
Ile-355
Arg-96
Arg-359

Figure 2. Noodleman's ten BS states (assuming C_3 symmetry of the cluster) with the net spin on each Fe ion indicated (up or down).[20] Without symmetry, BS3, BS4, BS6, BS7 and BS9 each split into three cases, whereas BS5, BS8 and BS10 split in six cases (obtained by permuting the spin on the Fe2–Fe4 and Fe5–Fe6 ions), giving a total of 35 BS states, studied in this paper. They were named with an extra number, e.g. BS3-1, BS3-2 and BS3-3 in an arbitrary, but consistent way, defined in Table S1.

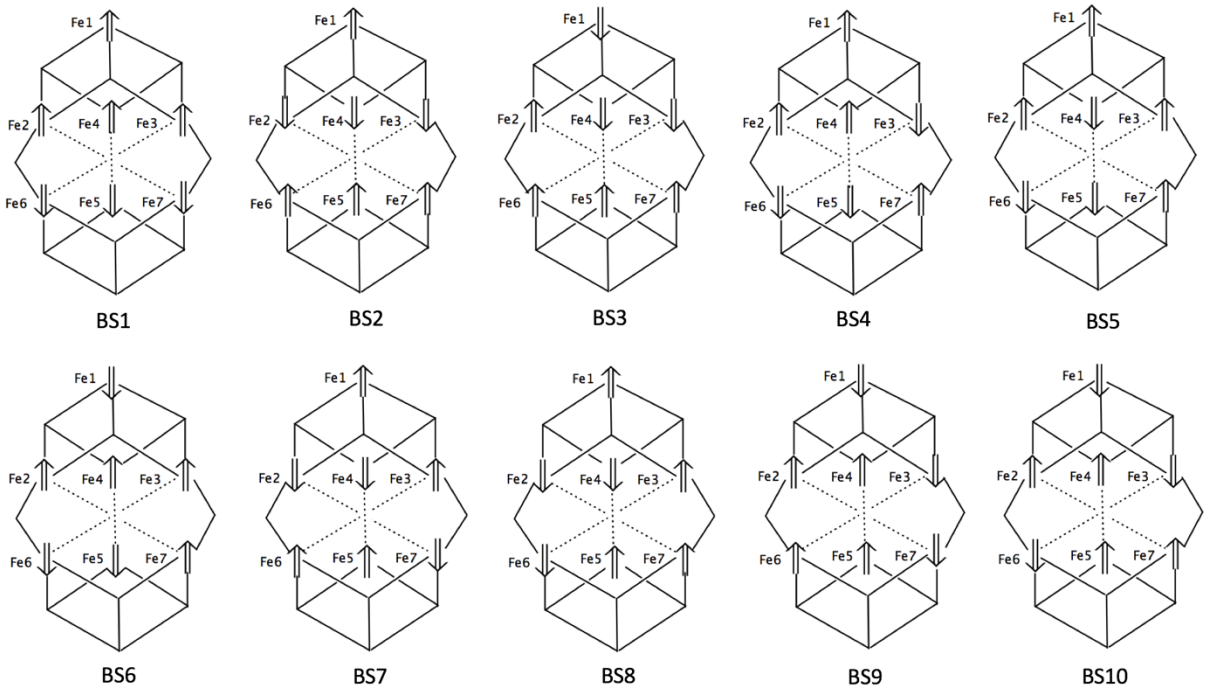

Figure 3. Spin state ordering of the quartet resting state in the individually QM/MM-optimised structures (with the TPSS-D3/def2-SV(P) method) obtained with the (a) TPSS-D3/def2-SV(P), (c) TPSS-D3/def2-TZVPD and (d) B3LYP/def2-TZVPD methods (the energy of the BS1 state, 268 kJ/mol, was truncated). In (b), the energies of the various BS states are calculated for the QM/MM-optimised structure of the BS7-1 state, with single-point energies with the TPSS-D3/def2-SV(P) method. On the *x*-axis, the BS states are sorted in the order BS1, BS2, BS3-1, BS3-2, BS3-3, BS4-1, BS4-2, …

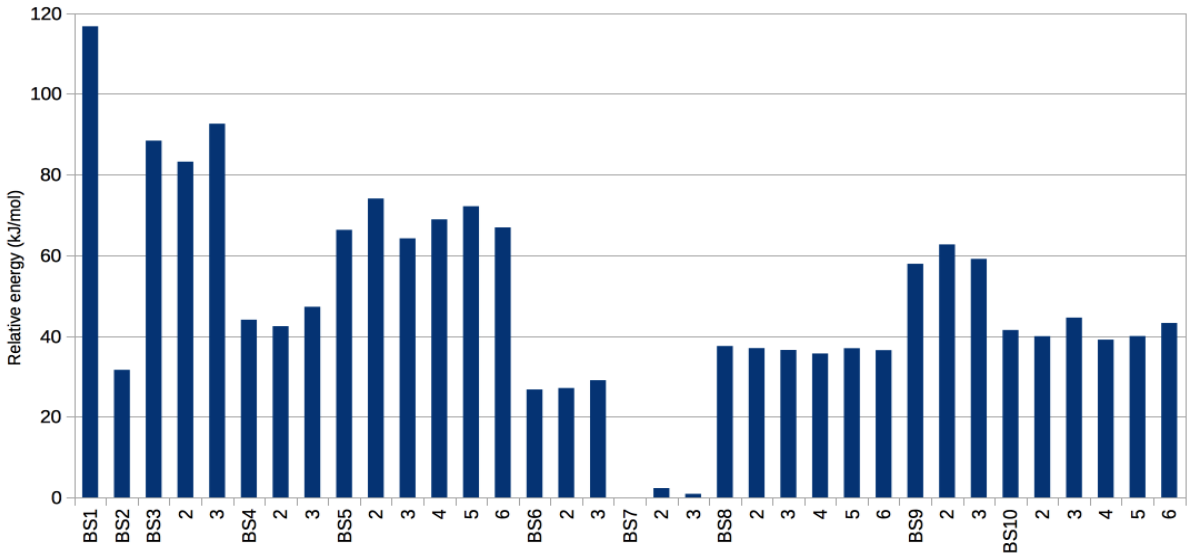

a

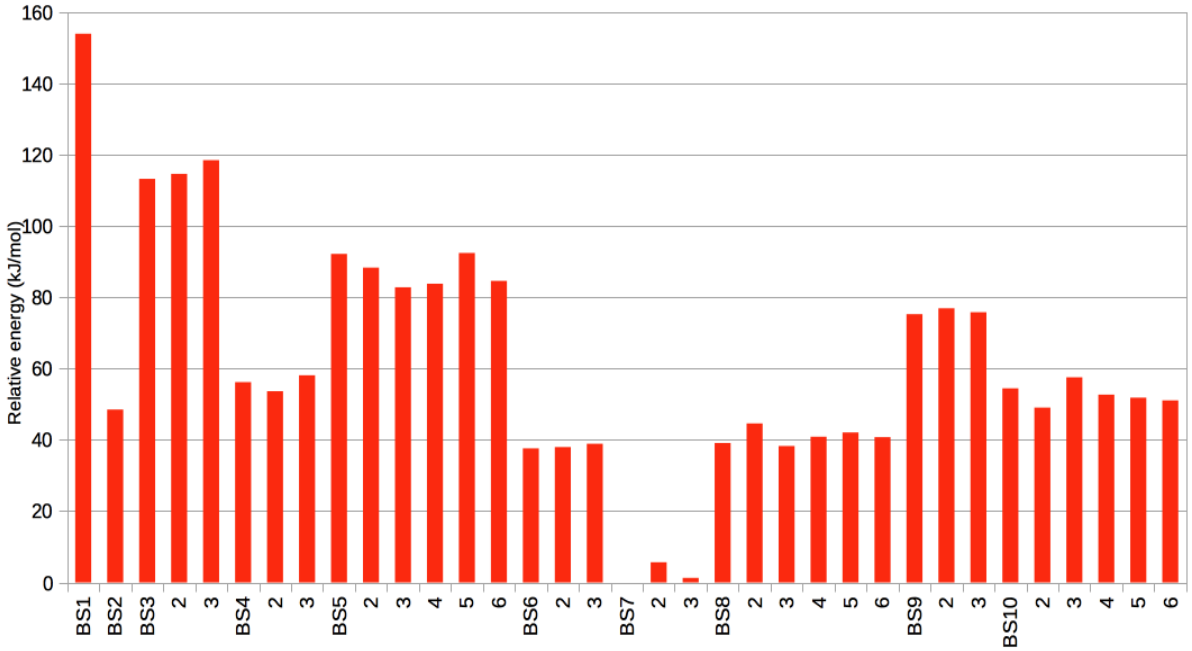

b

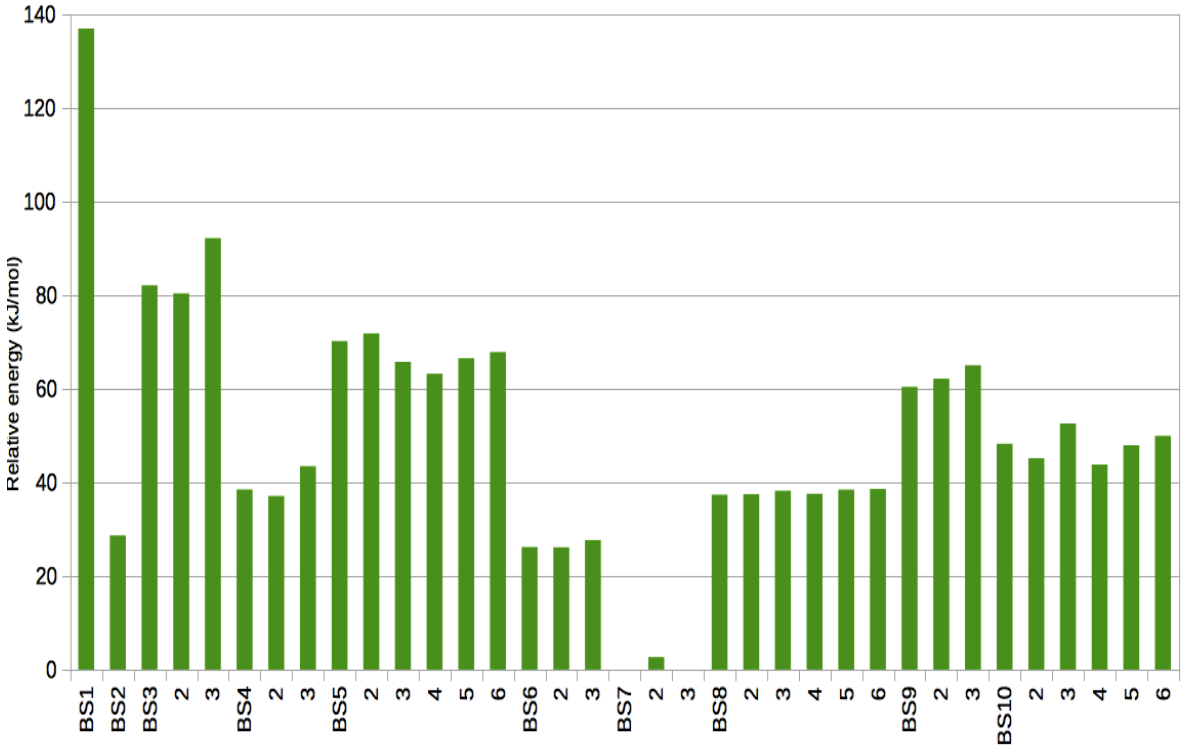
Relative energy (kJ/mol)
140
120
100
80
60
40
20
0
BS1 BS2 BS3 2 3 BS4 2 3 BS5 2 3 4 5 6 BS6 2 3 BS7 2 3 BS8 2 3 4 5 6 BS9 2 3 BS10 2 3 4 5 6

c

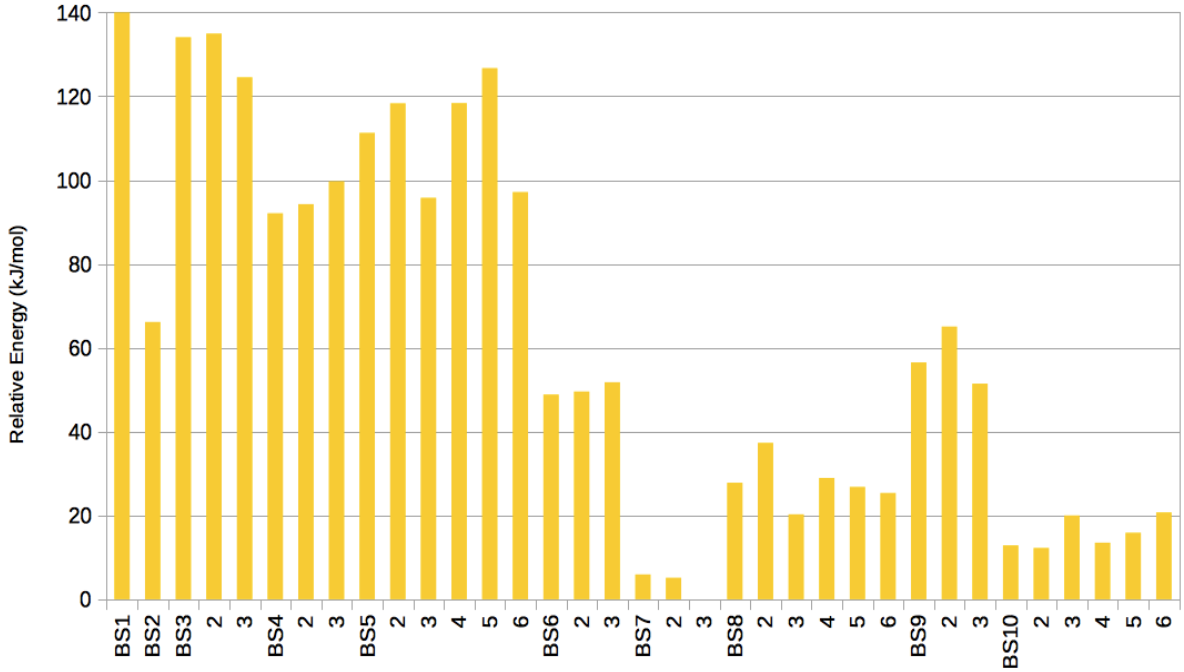
Relative Energy (kJ/mol)
140
120
100
80
60
40
20
0
BS1 BS2 BS3 2 3 BS4 2 3 BS5 2 3 4 5 6 BS6 2 3 BS7 2 3 BS8 2 3 4 5 6 BS9 2 3 BS10 2 3 4 5 6

d

Figure 4. Comparison of the optimised structure for the resting state of the FeMo cluster in the BS7-1 state, compared to the crystal structure of nitrogenase (in grey).[6]

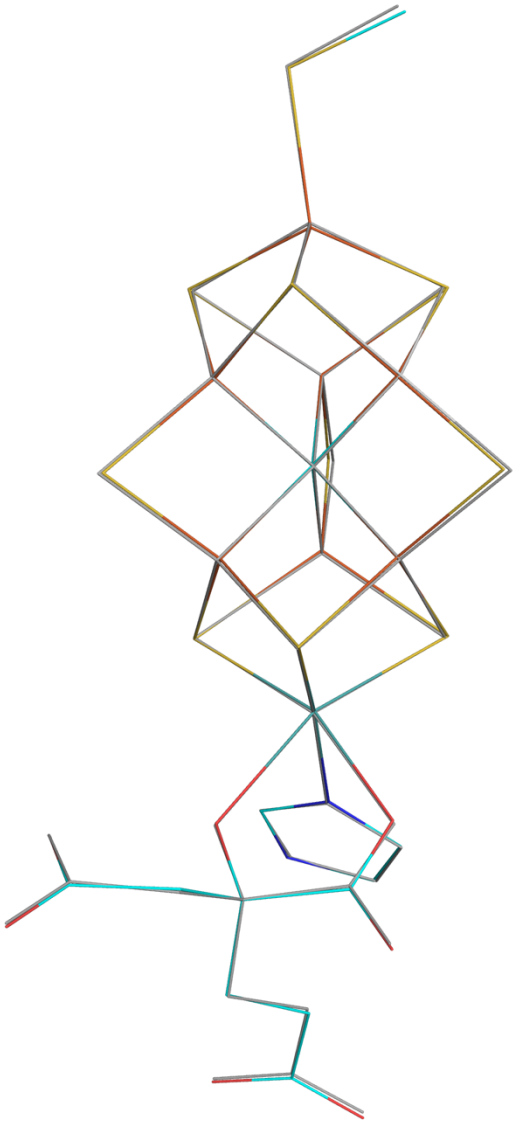

Figure 5. Spin state ordering of the doublet resting states in the individually QM/MM-optimised structures (with the TPSS-D3/def2-SV(P) method) obtained with the TPSS-D3/def2-SV(P) (SV), TPSS-D3/def2-TZVPD (TZ) and B3LYP-D3/def2-TZVPD methods, or at the QM/MM-optimised structure of the BS7-1 state, with single-point energies calculated with the TPSS-D3/def2-SV(P) method (SP). The reference energy is BS7-1 for the quartet state. BS1 with B3LYP has been truncated (312 kJ/mol).

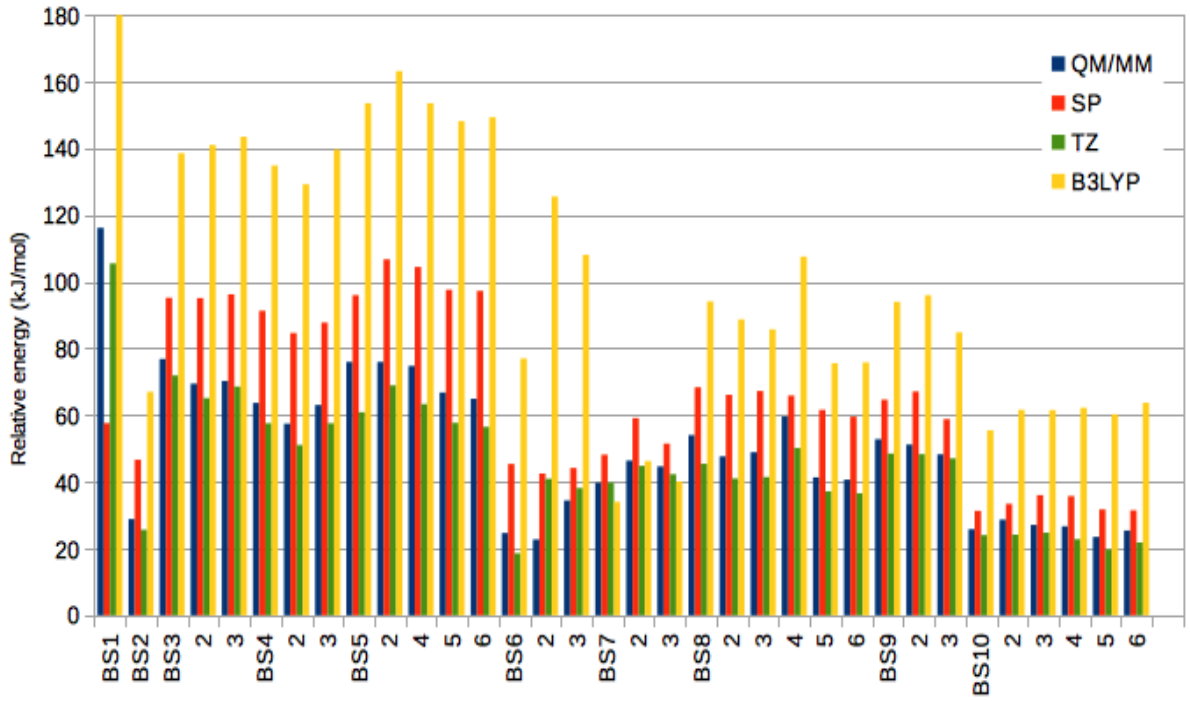

Figure 6. Spin state ordering of the (a) quintet, (b) triplet and (c) open-shell singlet reduced states for individually QM/MM-optimised structures (with the TPSS-D3/def2-SV(P) method) obtained with the TPSS-D3/def2-SV(P) (SV), TPSS-D3/def2-TZVPD (TZ) and B3LYP-D3/def2-TZVPD methods, or at the QM/MM-optimised structure of the resting BS7-1 state, with single-point energies calculated with the TPSS-D3/def2-SV(P) method (SP). The reference energy is that of BS7-1 for the quintet state. The B3LYP results for the BS1 state are truncated in b and c (277 and 270 kJ/mol, respectively).

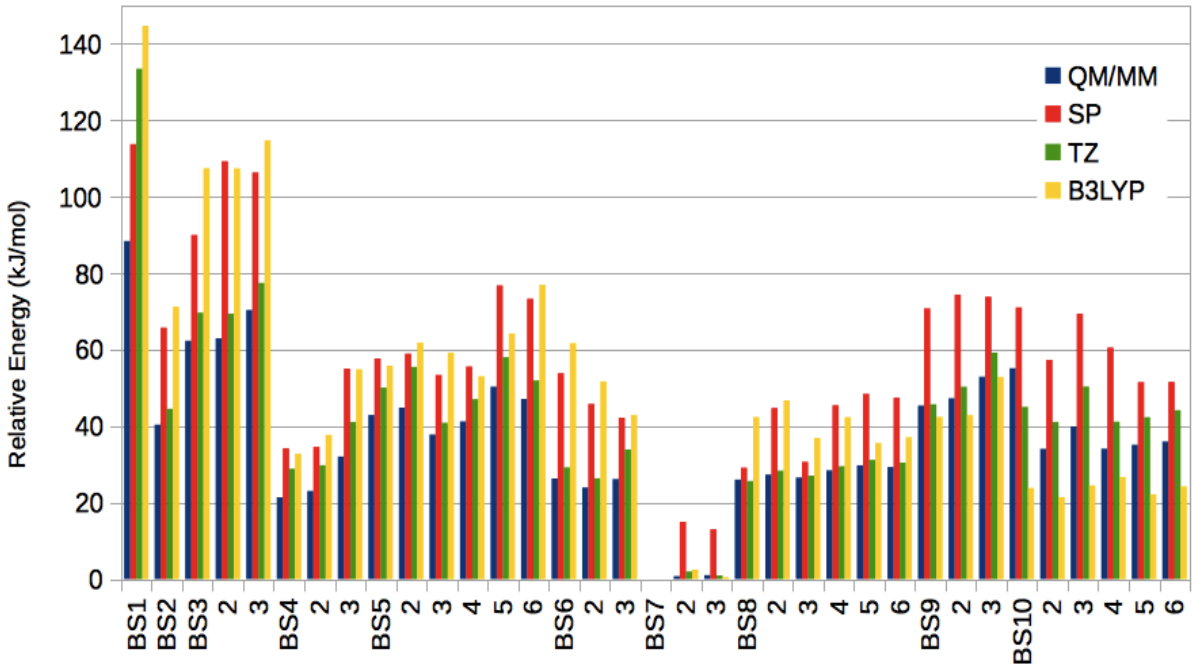

a

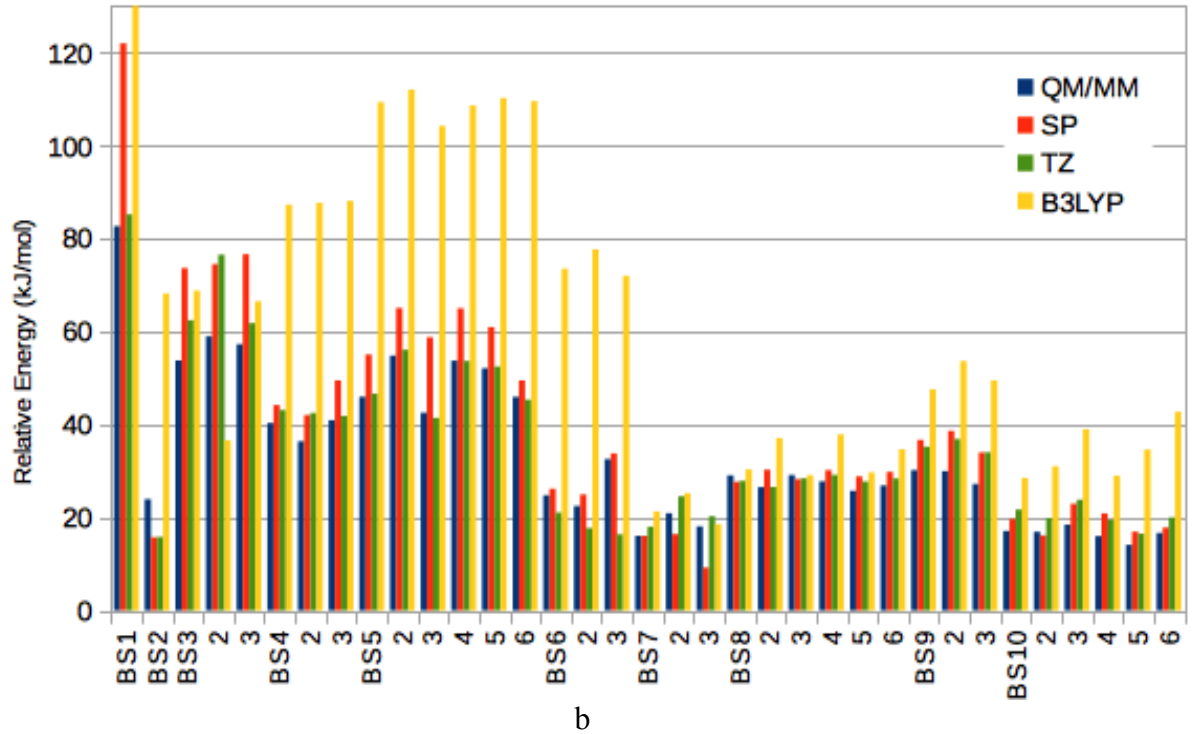

b

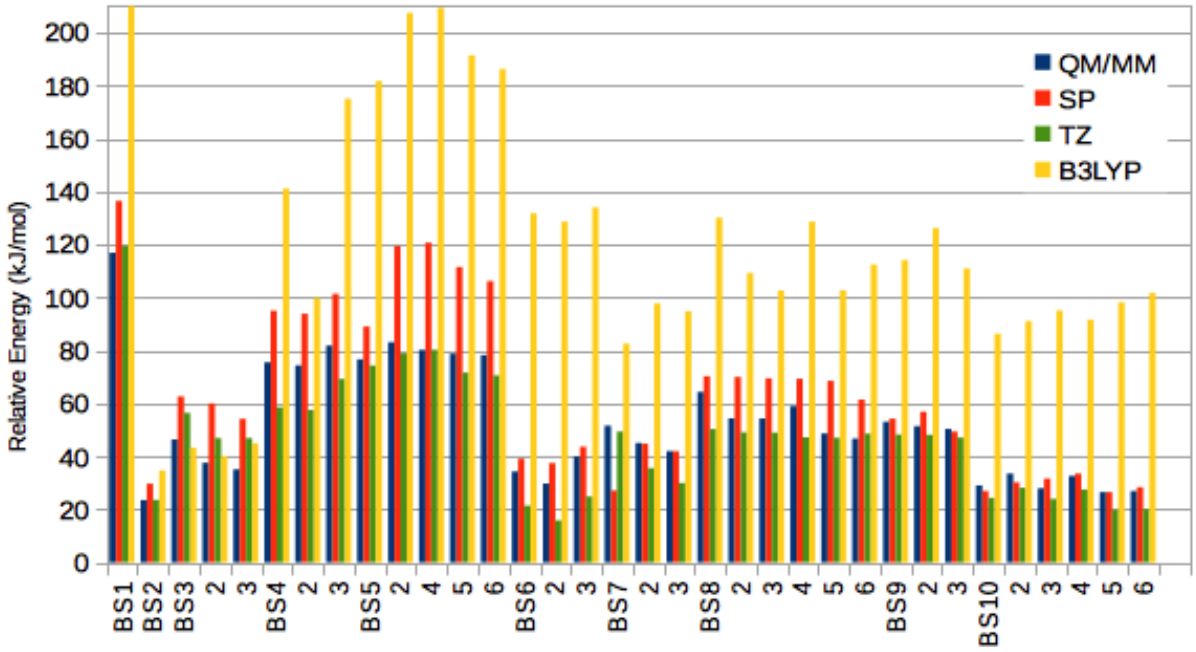
Relative Energy (kJ/mol)
200
180
160
140
120
100
80
60
40
20
0
QM/MM
SP
TZ
B3LYP
BS1
BS2
BS3
2
3
BS4
2
3
BS5
2
4
5
6
BS6
2
3
BS7
2
3
BS8
2
3
4
5
6
BS9
2
3
BS10
2
3
4
5
6

c

Figure 7. Spin state ordering of the quintet protonated state in the individually QM/MM-optimised structures (with the TPSS-D3/def2-SV(P) method) obtained with the TPSS-D3/def2-SV(P) (SV), TPSS-D3/def2-TZVPD (TZ) and B3LYP-D3/def2-TZVPD methods, or at the QM/MM-optimised structure of the BS7-1 state, with single-point energies calculated with the TPSS-D3/def2-SV(P) method (SP). The reference energy is the lowest BS7 state. The B3LYP result for BS1 has been truncated (293 kJ/mol).

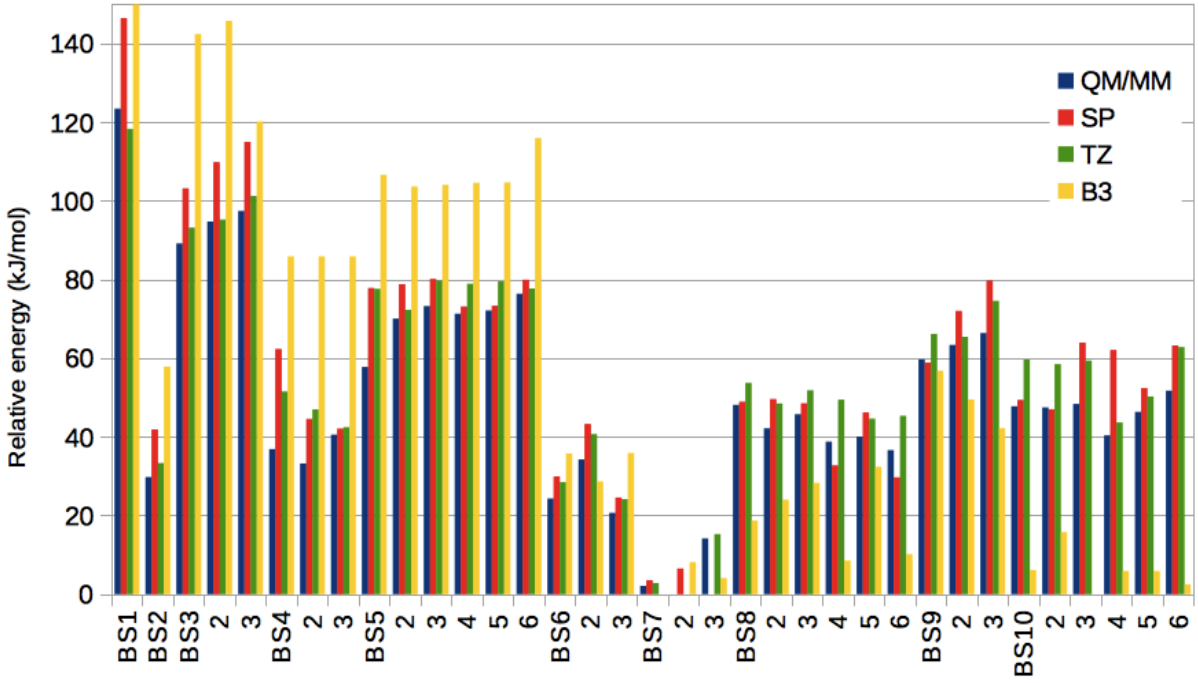

Figure 8. Spin state ordering of the doublet protonated state in the individually QM/MM-optimised structures (with the TPSS-D3/def2-SV(P) method) obtained with the TPSS-D3/def2-SV(P) (QM/MM) and B3LYP-D3/def2-SV(P) (B3) methods, or at the individually QM/MM-optimised structure of the quartet state, with single-point energies calculated with the TPSS-D3/def2-SV(P) method (SP).

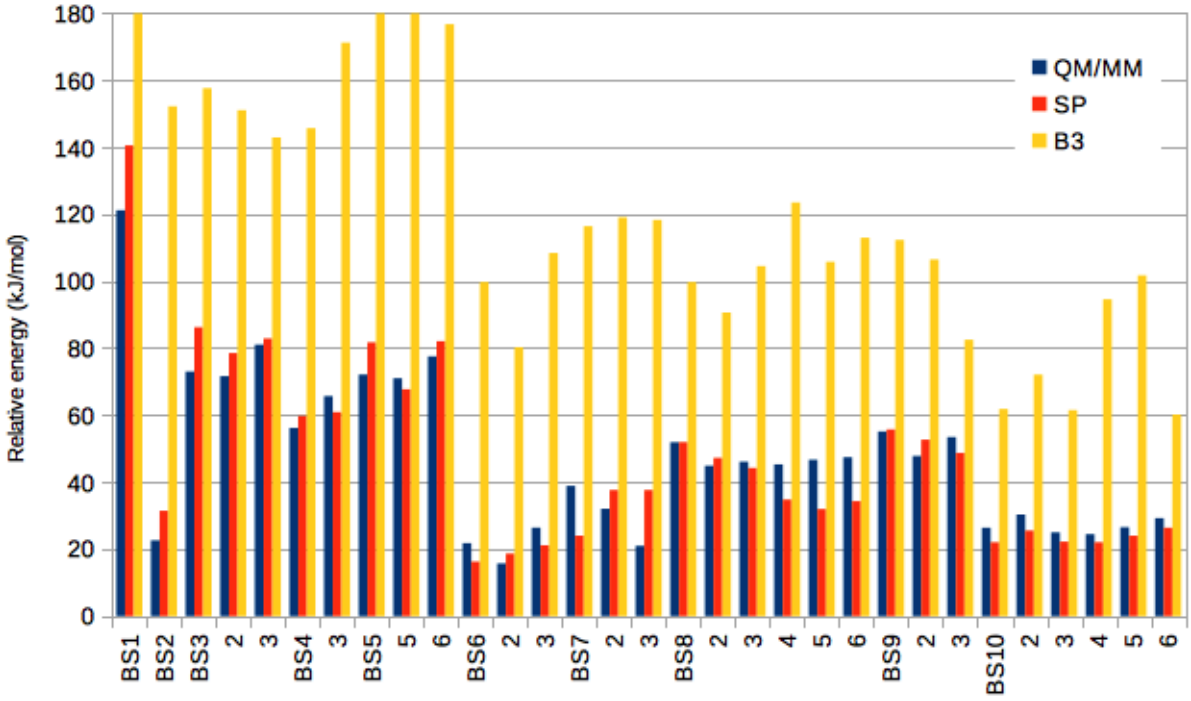

Figure 9. The QM model used in the protonated state with the added proton on the S2A atom. Distances to the Fe atoms are indicated (in Å).

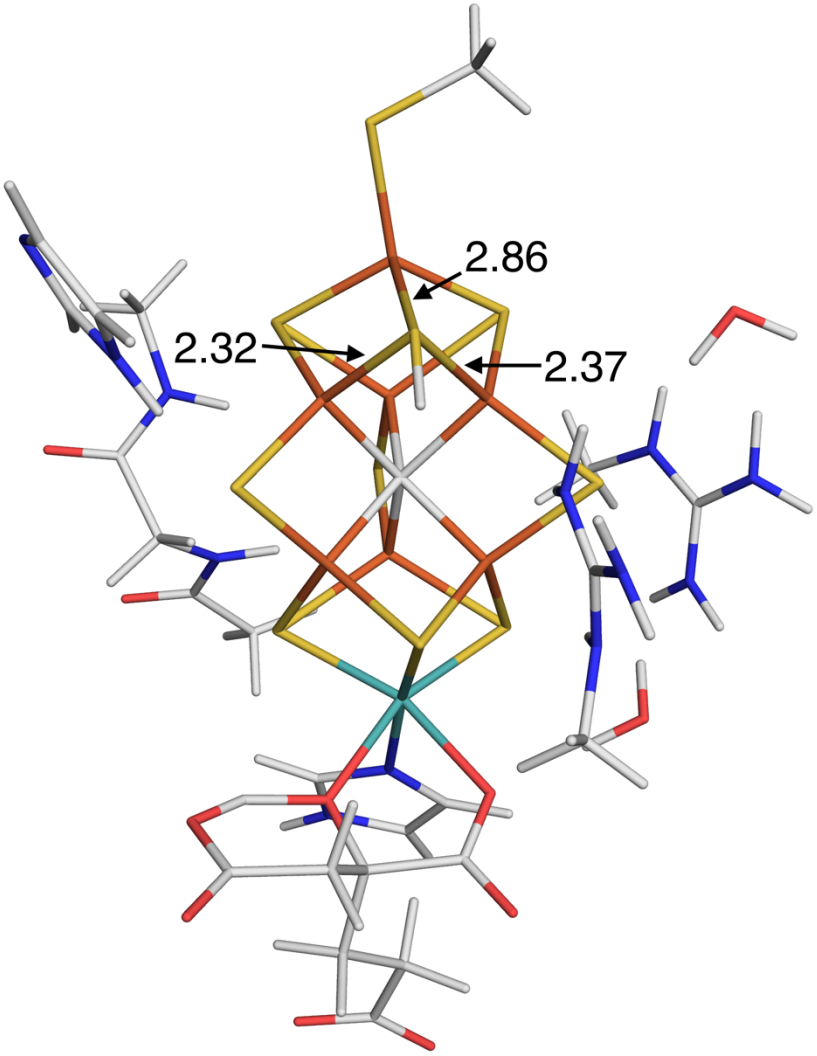

Figure 10. Spin state ordering of the quartet state protonated on S2A in the individually QM/MM-optimised structures (with the TPSS-D3/def2-SV(P) method) obtained with the TPSS-D3/def2-SV(P) (QM/MM) and B3LYP-D3/def2-SV(P) (B3) methods, or at the individually QM/MM-optimised structure of the quartet state, with single-point energies calculated with the TPSS-D3/def2-SV(P) method (SP). The reference energy is the lowest BS7 state. The B3LYP result for BS1 has been truncated (199 kJ/mol).